View metadata, citation and similar papers at core.ac.uk

brought to you by CORE

provided by Open Research Exeter

PROCEEDINGS OF SPIE

SPIEDigitalLibrary.org/conference-proceedings-of-spie

Role of defect states in functionalized graphene photodetectors

Jake D. Mehew
Matthew D. Barnes
Marc Dubois
Monica F. Craciun
Saverio Russo

SPIE.

Downloaded From: https://www.spiedigitallibrary.org/conference-proceedings-of-spie on 8/29/2017 Terms of Use: https://spiedigitallibrary.spie.org/ss/TermsOfUse.aspx

Role of defect states in functionalized graphene photodetectors

Jake D. Mehew[a,b], Matthew D. Barnes[b], Marc Dubois[c], Monica F. Craciun[b], Saverio Russo[b*]

[a]EPSRC Centre for Doctoral Training in Metamaterials (XM2), University of Exeter, Exeter EX4 4QL, UK; [b]Centre for Graphene Science, University of Exeter, Exeter EX4 4QL, UK; [c]Université Clermont Auvergne, ICCF UMR CNRS 6296, 63178 Aubière, France.

Abstract

The functionalization of graphene can enhance the optoelectronic properties of graphene, allowing the creation of highly sensitive broadband photodetectors. Presently, the role played by defects, induced by the functionalization of graphene, on the performance of graphene photodetectors is not well understood. Here, we investigate the optoelectronic properties of van der Waals heterostructures comprising of graphene and a functionalized partner, formed by pristine and fluorinated graphene. We find that the electrical properties of graphene are preserved upon formation of the heterostructure. A negligible charge transfer is observed across the interface between the two materials which limits the performance of the photodetector due to the vertical separation of the two materials.

Keywords: graphene, functionalized graphene, photodetector, defect states, fluorinated graphene

1. INTRODUCTION

The current interest in optoelectronic devices based on two-dimensional (2D) materials, such as graphene, stems from the additional functionalities that these materials possess, compared to those of established technologies. Their mechanical flexibility, for example, allows their integration as a transparent conductor onto textile fibers.[1],[2] Graphene field-effect transistors (FETs) can operate as high-speed photodetectors, with uniform light absorption across a broad spectral range.[3] However, their sensitivity to light is limited by the absence of a band gap, resulting in ultrafast recombination of photoexcited charges.

To engineer strong light absorption in graphene FETs various strategies have been put forward including the incorporation of plasmonic nanostructures[4] and the combination of graphene with semiconducting materials.[5][6][7] However, in these extrinsic strategies the spectral range of the photodetector is limited by the resonance of the plasmonic structure, or the absorption edge of the semiconductor which is typically in the visible, hindering their use in broadband photodetection applications.[3] Intrinsic strategies also exist whereby a band gap is opened in graphene through functionalization with adatoms, such as fluorine and hydrogen.[8],[9] This has been shown to increase the on/off current ratio in fluorinated graphene (FGr) FETs,[10],[11] far surpassing the negligible ratio found in pristine graphene FETs, opening the possibility for efficient graphene transistors for computing applications. Furthermore, demonstration of nanoscale patterning of fluorinated graphene by electron beam irradiation allows for further miniaturization of optoelectronic devices.[12]

The optical properties of fluorinated graphene have been widely investigated both experimentally, using absorption and photoluminescence spectroscopy,[13-15] and theoretically.[16] These works all indicate that the band gap of FGr can be tuned from the ultraviolet to near-infrared by controlling the degree of fluorination. Recently, a fluorinated graphene photodetector has been demonstrated with spectral range spanning 255 nm to 4.3 μm.[17] This broadband response arises from the quantum confinement of graphene regions by fluorine adatoms. In this experiment, the fluorination of only the top layer of a few-layer graphene is used to attain a self-aligned graphene/fluorinated graphene photo-active interface. However, in these structures it is not possible to truly identify whether the observed enhanced photoresponse is due to the defects induced by the fluorination process in the graphene under-layer and/or the energy gap of FGr. Furthermore, fluorine atoms have been shown to form clusters hundreds of nanometers in diameter on the graphene surface, as demonstrated by transmission electron microscopy studies,[18] leading to a high degree of non-uniformity in a micron-scaled device. At present, the role of fluorine clusters and defects induced in the graphene under-layer of a self-aligned Gr/FGr structure on the performance of photodetectors is unclear.

* s.russo@exeter.ac.uk

Active Photonic Platforms IX, edited by Ganapathi S. Subramania, Stavroula Foteinopoulou, Proc. of SPIE Vol. 10345, 103450V · © 2017 SPIE · CCC code: 0277-786X/17/$18 · doi: 10.1117/12.2273987

Downloaded From: https://www.spiedigitallibrary.org/conference-proceedings-of-spie on 8/29/2017 Terms of Use: https://spiedigitallibrary.spie.org/ss/TermsOfUse.aspx

In this work, we study the effect of fluorine functionalization on the photosensitivity of a graphene transistor through electrical transport measurements, combined with complementary photocurrent and Raman mapping. We chose to assemble functionalized graphene photodetectors by mechanically transferring graphene onto FGr. This fabrication procedure eliminated potential spurious defect states induced by the functionalization of the top layers in a self-aligned photodetector.

2. FABRICATION

Graphene-FGr heterostructure photodetectors were fabricated on p-Si/SiO_2 (290 nm) substrates, where the highly doped silicon serves as a back gate. FGr was mechanically exfoliated from bulk fluorinated graphite using the scotch tape method. As previously demonstrated,[10][11] to achieve a wide range in the degree of fluorination two routes were employed, one in which graphite was heated in a molecular fluorine, F_2, atmosphere at high temperatures (>300 ^oC), and the other where graphite was exposed to XeF_2 gas (xenon difluoride) at lower temperatures (120 ^oC) thanks to the XeF_2 (s) = XeF_2 (s) equilibrium (crystals of XeF_2 were added to graphite flakes in a closed reactor in Ar atmosphere of a glove box). XeF_2 releases atomic fluorine which allows homogenous dispersion of fluorine into the graphite lattice to be achieved; mechanical exfoliation is then efficient to prepare mono- and few-layer FGr. High quality graphene grown by -chemical vapor deposition (CVD) was then transferred onto the FGr using an electrochemical delamination technique, with conductive graphene channels defined by electron beam lithography and O_2 plasma etching. An additional electron beam lithography step was used to define electrical contacts before metallization by thermal evaporation of Cr/Au (5/60 nm) and subsequent lift-off in n-methyl-2-pyrrolidone. Figure 1a shows a schematic of the device structure with the electrical connections used for electrical characterization. A graphene FET was fabricated adjacent to the graphene-FGr device, which serves as a reference, as seen in the optical micrograph in Figure 1b.

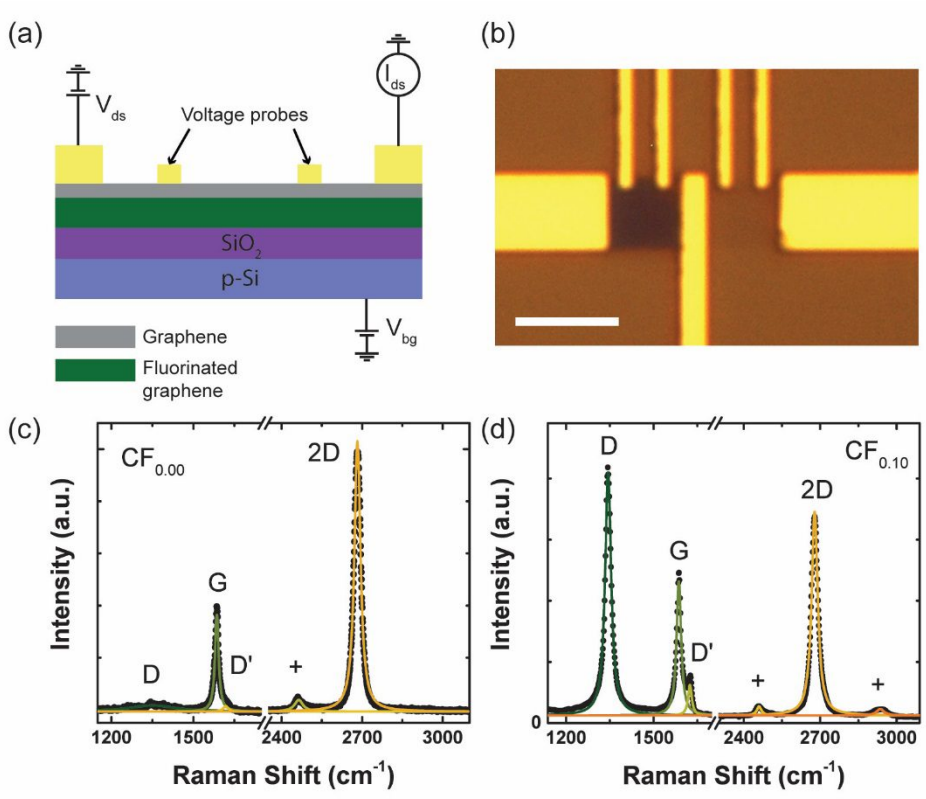

Figure 1. (a) Schematic of graphene/fluorinated graphene (FG) heterostructure device with electrical connections included. (b) Optical micrograph of Gr/FG device with the adjacent Gr device providing a reference sample. Scale bar is 4 μm. (c,d) Raman spectra of graphene (c), and fluorinated graphene (d) single layers. The peaks labelled + represent multiple phonon modes.

Downloaded From: https://www.spiedigitallibrary.org/conference-proceedings-of-spie on 8/29/2017 Terms of Use: https://spiedigitallibrary.spie.org/ss/TermsOfUse.aspx

Raman spectroscopy is a non-destructive tool used for the characterization of graphene and FGr flakes.[19] From the spectra in Figures 1c and 1d multiple features can be identified by Lorentzian fits as the G, D, D', and 2D peaks of graphene. The position and relative intensity of these peaks contain information about a number of material properties including level of doping, degree of disorder, and electronic quality. The G peak (~1580 cm^{-1}) is attributed to the degenerate high frequency E_{2g} phonon found at the center of the Brillioun zone (Γ) and can be observed in any sp^2-hybridised carbon. Two additional peaks are observed around 1350 and 1620 cm^{-1}, labelled D and D' respectively.

Disruption of the sp^2 network of carbon is required for these peaks to appear and in graphene one would normally only expect to observe the D peak in regions close to the edge of flakes, where the high density of structural defects breaks the translational symmetry. Indeed, the low I(D)/I(G) and I(D')/I(G) ratios seen in Figure 1c are indicative of the high crystalline quality of graphene. During fluorination there is a change from sp^2 to sp^3 hybridization, as fluorine adatoms are covalently grafted onto the graphene lattice. The increase in the intensities of these defect peaks, Figure 1d, can be attributed to the presence of these fluorine adatoms. The 2D peak (~2700 cm^{-1}) involves two inter-valley phonons at the K point, with this second order process not requiring disorder or defects for it to be active. Fitting of this peak with a single Lorentzian is an indication that the graphene is a single layer.

3. OPTOELECTRONIC CHARACTERIZATION

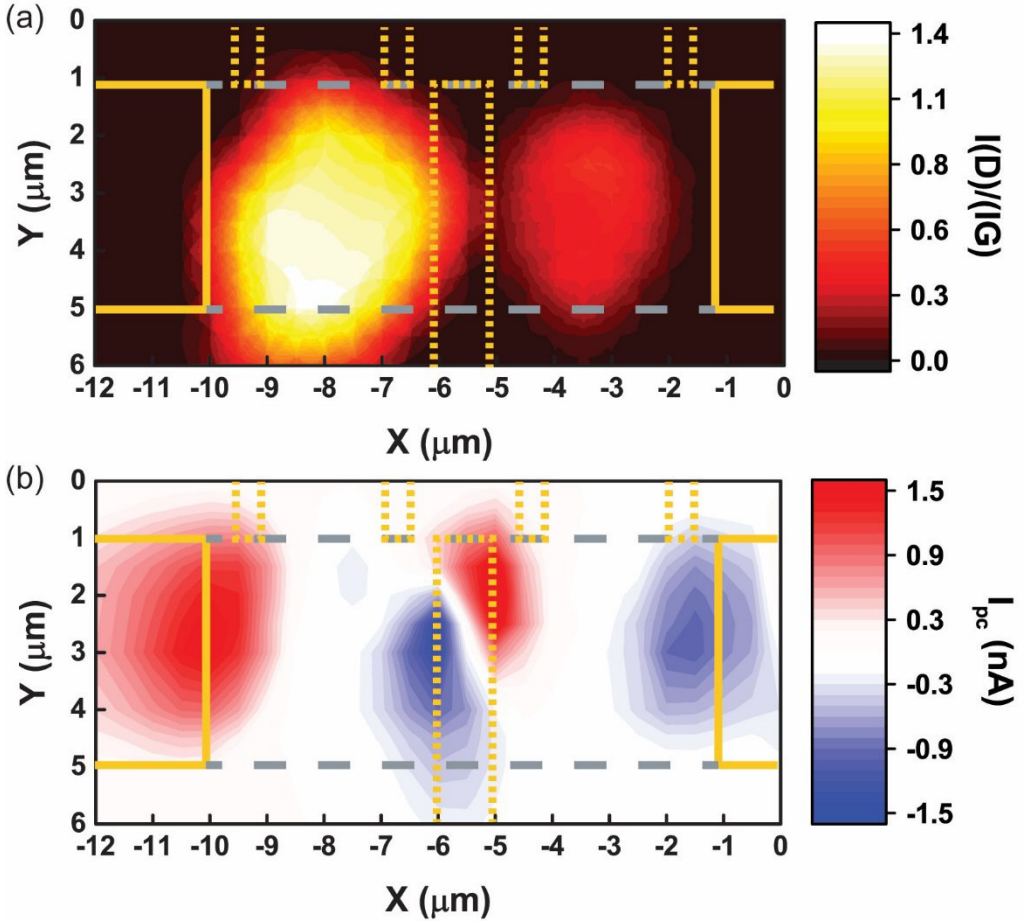

Figure 2. (a) Raman map of the intensity ratio of the D and G peaks across graphene-FGr and graphene regions (514 nm, 1.2 mW). The grey dashed line outlines the CVD graphene region and the yellow lines the Cr/Au electrodes. (b) Corresponding photocurrent map (473 nm, 48.6 μW). The solid yellow lines are the electrodes used in acquiring this measurement.

To probe the optoelectronic properties of the device with sub-micron resolution we used a home-built optical microscope which has the capability to perform a range of optoelectronic measurements, including photocurrent and Raman

Downloaded From: https://www.spiedigitallibrary.org/conference-proceedings-of-spie on 8/29/2017 Terms of Use: https://spiedigitallibrary.spie.org/ss/TermsOfUse.aspx

mapping.[20] Figure 2a shows a Raman map of the intensity ratio of the D and G peaks, I(D)/I(G), acquired across both graphene/FGr and graphene regions of the same device. The brightest regions have the highest I(D)/I(G) value and provide a visualization to the presence of FGr. As detailed above, the adsorption of fluorine onto the graphene lattice changes the hybridization of electronic orbitals from sp^2 to sp^3 configuration resulting in an increased D peak intensity. In regions of graphene on SiO_2 a non-zero I(D)/I(G) ratio is also observed which likely arises at grain boundaries formed in the CVD growth of graphene. Nevertheless, the higher intensity ratio in the graphene/FGr region confirms the presence of fluorinated graphene.

Figure 2b shows a photocurrent map of this region, where a modulated laser beam (473 nm, 48.6 μW) is rastered across the sample with the resulting signal recorded on a lock-in amplifier. The map reveals the presence of hot spots, where the photocurrent is non-zero, located in the proximity of the metal electrodes which are known to be due to the photo-thermoelectric effect.[21] In both device structures, as the laser moves towards the center of the channel the signal quickly diminishes. Clearly, as no correlation can be seen between the Raman and photocurrent maps the role of FGr in these heterostructure photodetectors remains uncertain.

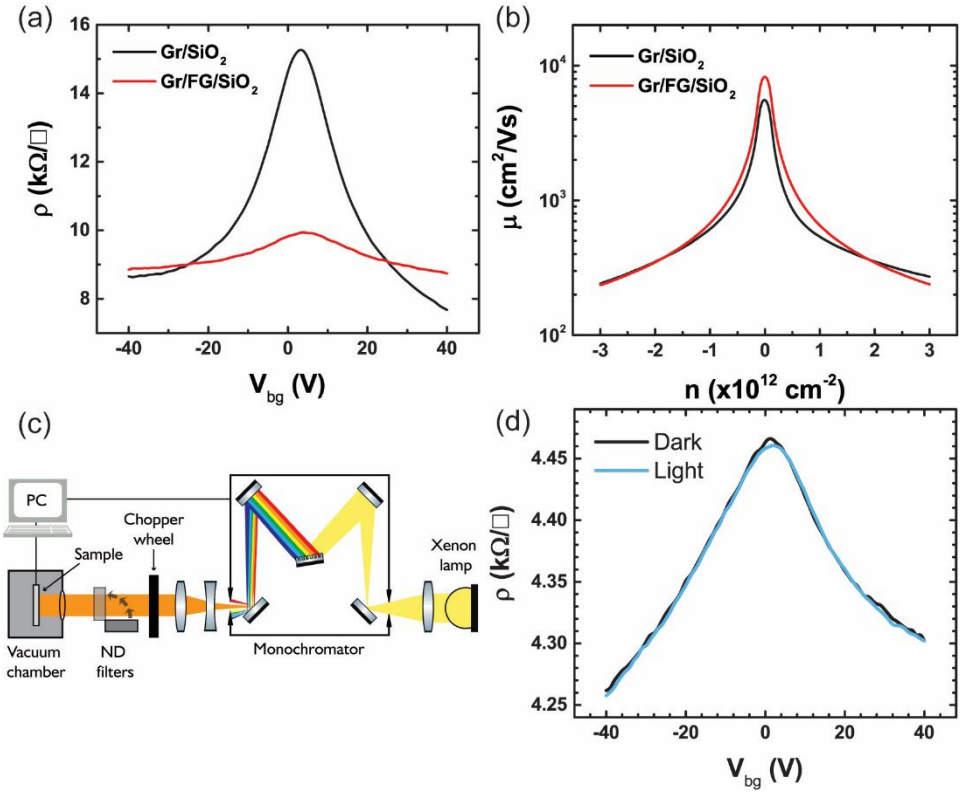

Figure 3. (a) Two-terminal channel resistivity (ρ) versus applied gate voltage (V_{bg}) for graphene on SiO_2 and graphene/FG on SiO_2. (b) Field effect mobility (μ) versus carrier concentration (n) extracted from the transfer curves in (a). (c) Schematic of a home-built vacuum chamber with tunable light source for optoelectronic characterization. (d) Four-terminal gate dependent resistivity in dark and under illumination (400 nm, 4.2 mW/cm^2).

To gain insight into the role of FGr on the performance of the photodetector we investigate the electrical properties of the graphene channel. Figure 3a shows the gate voltage dependence of the resistivity of graphene. The application of a positive (negative) gate voltage induces electrons (holes) in the graphene channel with this ambipolar behavior typical of graphene. In the graphene-FGr heterostructure device the peak in resistivity (~10 kΩ/sq) is smaller than that of the reference graphene FET (~15 kΩ/sq). This can be understood as a screening of the electric field felt by the graphene channel by the presence of the fluorinated graphene underneath, diminishing the ability to deplete the channel. Crucially, there appears to be no charge transfer between graphene and FGr, as exhibited by the absence of a shift in Dirac point, located in both cases at V_{bg} = +3 V. The mobility of the graphene channel can be extracted from the gate dependent resistivity using the parallel plate capacitor model, see Figure 3b. In both cases, the mobility peaks around the Dirac point and decays with increasing carrier concentration. At a carrier concentration of 1x10^{12} cm^{-2} the hole (electron)

Downloaded From: https://www.spiedigitallibrary.org/conference-proceedings-of-spie on 8/29/2017 Terms of Use: https://spiedigitallibrary.spie.org/ss/TermsOfUse.aspx

mobility is calculated to be 645 (623) and 590 (521) cm^2/Vs for the device structure with and without FGr respectively. The slight increase in mobility for the graphene-FGr device could arise from reduced charge carrier scattering with charged impurities in the SiO_2, as a result of the aforementioned screening effect.

To characterize the photogeneration mechanisms in graphene-FGr heterostructure the devices were transferred into a home-built vacuum chamber (10^{-7} mbar), see Figure 3c. A xenon lamp, monochromator, and collimating optics (Oriel TLS-300X) were used to provide an incident light source in the spectral range 300 nm to 1.8 μm. Neutral density (ND) filters and a motorized chopper wheel were used to attenuate and modulate the signal respectively. Figure 3d shows the four-terminal transfer curves (V_{ds} = 100 mV) of the graphene-FGr device acquired in both dark and light (400 nm, 4.2 mW/cm^2) conditions. It is apparent that there is a negligible change in the resistivity of the graphene channel under illumination, across a wide range of applied gate voltages. One would expect that light absorption in fluorinated graphene would generate electron-hole pairs, with one charge carrier transferred to the graphene channel and the other remaining trapped within FGr, following a mechanism of charge excitation and transfer observed in semiconductor/graphene photodetectors.[5]-[7] This would manifest as a shift in the Dirac point under illumination. The absence of shift leads to two possible conclusions: firstly that FGr is transparent at these wavelength, or that there is absorption in FGr but limited charge transfer between graphene and FGr. The former can be eliminated as absorption measurements of FGr with a similar fluorine content (19%) demonstrated a band gap of 2.48 eV,[15] well below the photon energy used here (3.1 eV).

The transfer curves acquired in dark and under illumination show no discernible charge transfer between FGr and graphene. In the recent work of Du et al.,[17] they devised an alternative structure whereby few-layer CVD graphene was fluorinated in an inductively coupled SF_6 plasma. The decomposition of SF_6 into atomic fluorine, and subsequent grafting onto graphene, predominately takes place in the uppermost layers. Contrary to the van der Waals stack FGr/graphene photodetector studied in this work, the self-aligned functionalized structures studied by Du et al. have been found to show a considerable improvement of the photoresponse. The microscopic origin of the difference in the performance resides in the presence of defect states in the graphene layer. More specifically, the plasma fluorination results in a non-uniform functionalization with a pristine under-layer of graphene. Due to the high electronegativity of fluorine, the presence of sparse adatoms introduces trap sites which can hold a photo-excited electron (hole) while the other charge type, that is hole (electron), is recirculated in graphene leading to a net gain mechanism. In our van der Waals FGr/Gr photodetectors the conductive underlying graphene channel is never exposed to the harsh conditions of the functionalization, leading to a drastic reduction of trap sites. Hence, our findings show that the role of defects states in functionalized graphene photodetectors needs to be fully clarified. Further work on theoretical modelling of the defect states and transient current studies of the relaxation times for a wide range of defects will be necessary to optimize the photoresponse of functionalized graphene transistors.[22]

4. CONCLUSIONS

In summary, we have characterized the optoelectronic properties of graphene-FGr heterostructure photodetectors. Raman spectroscopy and scanning photocurrent microscopy techniques were employed in an attempt to correlate the presence of fluorinated graphene to the photocurrent generated in our devices. Fluorine adatoms, identified by the presence of the D peak in the Raman map, have a negligible contribution to the spatial dependence of the photocurrent. In addition, the transfer curves of graphene/FGr in dark, and under illumination, showed no charge transfer at the interface between graphene and fluorinated graphene. This result is in contrast with a previous study which showed a considerable improvement in the photoresponse of a graphene/FGr device. We attribute this discrepancy to a difference in the density of defect-induced trap states between the two device structures. Further work is necessary to determine the precise role of these defect states in functionalized graphene photodetectors.

5. ACKNOWLEDGEMENTS

The authors thank Adolfo De Sanctis for his assistance in obtaining the Raman maps and for useful discussions. J.D.M. acknowledges financial support from the Engineering and Physical Sciences Research Council (EPSRC) of the United

Downloaded From: https://www.spiedigitallibrary.org/conference-proceedings-of-spie on 8/29/2017 Terms of Use: https://spiedigitallibrary.spie.org/ss/TermsOfUse.aspx

Kingdom, via the EPSRC Centre for Doctoral Training in Metamaterials (Grant No. EP/L015331/1). S.R. and M.F.C. acknowledge financial support from EPSRC (Grant No. EP/J000396/1, EP/K017160/1, EP/K010050/1, EP/ G036101/1, EP/M001024/1, and EP/M002438/1) and from Royal Society International Exchanges Scheme 2016/R1.

REFERENCES

[1] Neves, A. I. S., Bointon, T. H., Melo, L. V., Russo, S., de Schrijver, I., Craciun, M. F.., Alves, H., "Transparent conductive graphene textile fibers," Sci. Rep. 5, 9866 (2015).
[2] Neves, A. I. S., Rodrigues, D. P., De Sanctis, A., Alonso, E. T., Pereira, M. S., Amaral, V. S., Melo, L. V., Russo, S., de Schrijver, I., Alves, H, and Craciun M. F., "Towards conductive textiles: coating polymeric fibres with graphene," Sci. Rep. 7(1), 4250 (2017).
[3] Koppens, F. H., Mueller, T., Avouris, P., Ferrari, a C., Vitiello, M. S.., Polini, M., "Photodetectors based on graphene, other two-dimensional materials and hybrid systems," Nat Nanotechnol 9(10), 780–793 (2014).
[4] Echtermeyer, T. J., Britnell, L., Jasnos, P. K., Lombardo, A., Gorbachev, R. V., Grigorenko, A. N., Geim, A. K., Ferrari, A. C., Novoselov, K. S., "Strong plasmonic enhancement of photovoltage in graphene," Nat. Commun. 2, 458 (2011).
[5] Mehew, J. D., Unal, S., Torres Alonso, E., Jones, G. F., Fadhil Ramadhan, S., Craciun, M. F., Russo, S., "Fast and Highly Sensitive Ionic-Polymer-Gated WS2-Graphene Photodetectors," Adv. Mater. 29(23), 1700222 (2017).
[6] Konstantatos, G., Badioli, M., Gaudreau, L., Osmond, J., Bernechea, M., de Arquer, F. P. G., Gatti, F., Koppens, F. H. L., "Hybrid graphene–quantum dot phototransistors with ultrahigh gain," Nat. Nanotechnol. 7(6), 363–368 (2012).
[7] Roy, K., Padmanabhan, M., Goswami, S., Sai, T. P., Ramalingam, G., Raghavan, S., Ghosh, A., "Graphene–MoS2 hybrid structures for multifunctional photoresponsive memory devices," Nat. Nanotechnol. 8(11), 826–830 (2013).
[8] Elias, D. C., Nair, R. R., Mohiuddin, T. M. G., Morozov, S. V., Blake, P., Halsall, M. P., Ferrari, A. C., Boukhvalov, D. W., Katsnelson, M. I., et al., "Control of graphene's properties by reversible hydrogenation: evidence for graphane.," Science 323(5914), 610–613 (2009).
[9] Robinson, J. T., Burgess, J. S., Junkermeier, C. E., Badescu, S. C., Reinecke, T. L., Perkins, F. K., Zalalutdniov, M. K., Baldwin, J. W., Culbertson, J. C., et al., "Properties of fluorinated graphene films," Nano Lett. 10(8), 3001–3005 (2010).
[10] Withers, F., Dubois, M., Savchenko, A. K., "Electronic properties of fluorinated single-layer graphene transistors," Phys. Rev. B - Condens. Matter Mater. Phys. 82(7), 73403 (2010).
[11] Withers, F., Russo, S., Dubois, M., Craciun, M. F., "Tuning the electronic transport properties of graphene through functionalisation with fluorine," Nanoscale Res. Lett. 6(1), 526 (2011).
[12] Withers, F., Bointon, T. H., Dubois, M., Russo, S., Craciun, M. F., "Nanopatterning of fluorinated graphene by electron beam irradiation," Nano Lett. 11(9), 3912–3916 (2011).
[13] Wang, B., Sparks, J. R., Gutierrez, H. R., Okino, F., Hao, Q., Tang, Y., Crespi, V. H., Sofo, J. O., Zhu, J., "Photoluminescence from nanocrystalline graphite monofluoride," Appl. Phys. Lett. 97(14), 1–4 (2010).
[14] Jeon, K. J., Lee, Z., Pollak, E., Moreschini, L., Bostwick, A., Park, C. M., Mendelsberg, R., Radmilovic, V., Kostecki, R., et al., "Fluorographene: A wide bandgap semiconductor with ultraviolet luminescence," ACS Nano 5(2), 1042–1046 (2011).
[15] Ho, K. I., Liao, J. H., Huang, C. H., Hsu, C. L., Zhang, W., Lu, A. Y., Li, L. J., Lai, C. S., Su, C. Y., "One-step formation of a single atomic-layer transistor by the selective fluorination of a graphene film," Small 10(5), 989–997 (2014).
[16] Wei, W., Jacob, T., "Electronic and optical properties of fluorinated graphene: A many-body perturbation theory study," Phys. Rev. B 87(11), 115431 (2013).
[17] Du, S., Lu, W., Ali, A., Zhao, P., Shehzad, K., Guo, H., Ma, L., Liu, X., Pi, X., et al., "A Broadband Fluorographene Photodetector," Adv. Mater. 29(22), 1700463 (2017).
[18] Kashtiban, R. J., Dyson, M. A., Nair, R. R., Zan, R., Wong, S. L., Ramasse, Q., Geim, A. K., Bangert, U., Sloan, J., "Atomically resolved imaging of highly ordered alternating fluorinated graphene," Nat. Commun. 5(1), 4902 (2014).

Downloaded From: https://www.spiedigitallibrary.org/conference-proceedings-of-spie on 8/29/2017 Terms of Use: https://spiedigitallibrary.spie.org/ss/TermsOfUse.aspx

[19] Ferrari, A. C., Basko, D. M., “Raman spectroscopy as a versatile tool for studying the properties of graphene,” Nat. Nanotechnol. 8(4), 235–246 (2013).
[20] De Sanctis, A., Jones, G. F., Townsend, N. J., Craciun, M. F., Russo, S., “An integrated and multi-purpose microscope for the characterization of atomically thin optoelectronic devices,” Rev. Sci. Instrum. 88(5), 55102 (2017).
[21] De Sanctis, A., Jones, G. F., Wehenkel, D. J., Bezares, F., Koppens, F. H. L., Craciun, M. F., Russo, S., “Extraordinary linear dynamic range in laser-defined functionalized graphene photodetectors,” Sci. Adv. 3(5), e1602617 (2017).
[22] Amit, I., Octon, T. J., Townsend, N. J., Reale, F., Wright, C. D., Mattevi, C., Craciun, M. F., Russo, S., “Role of Charge Traps in the Performance of Atomically Thin Transistors,” Adv. Mater. 29(19), 1605598 (2017).

Downloaded From: https://www.spiedigitallibrary.org/conference-proceedings-of-spie on 8/29/2017 Terms of Use: https://spiedigitallibrary.spie.org/ss/TermsOfUse.aspx